Precoding and Receiver Processing for Multiple Access MIMO FBMC Systems

Madushanka Soysa
Department of Electrical and Computer Engineering,
University of California at San Diego,
La Jolla, CA
E-mail: msoysa@ucsd.edu

Nandana Rajatheva, and Matti Latva-aho
Department of Communication Engineering,
University of Oulu,
Finland
E-mail: rrajathe@ee.oulu.fi, matti.latva-aho@ee.oulu.fi

***Abstract*—Different transceiver processing methods are considered for filter bank multicarrier (FBMC) multiple access MIMO system. FBMC is considered a contender as an access method for 5G due to better spectral properties without the loss of data rate incurred by the presence of cyclic prefix in comparison to OFDM. Flexible spectrum utilization and possibility of using different pulse shapes for a variety of scenarios makes it an attractive option. However, the main challenge in FBMC systems is the presence of intersymbol interference (ISI) and intercarrier inteference (ICI). This makes the receiver performance to be degraded without suitable methods to mitigate those effects especially in the case of MIMO systems where there is a significant need for further investigation. We consider synchronous uplink and downlink multiple access with different processing techniques to alleviate interference. Results show that for the uplink we need to employ forward error correction in addition to receiver processing to obtain acceptable performance levels. With channel state and all users information available, the downlink produces better bit error rates (BER) comparatively.**

***Index Terms* - Filter bank; OQAM; receiver processing; precoding; multiple access**

I. Introduction

Future wireless systems are expected to integrate a variety of scenarios from vehicular, machine type communication (MTC) and the normal person to person case. Depending on each, there is a significant demand to have high rate video download-upload, real time gaming and others. These fuel the continued investigation for bandwidth and spectrally efficient access techniques and also for flexible spectrum usage. The traditional and well established OFDM waveform [1] exhibits significant leakage and would be particularly disadvantageous in the expected unsyncrhonized cognitive radio systems. The filterbank based systems on the other hand have a longer pulse shape producing a compact and fast decaying subcarrier spectrum. The absence of a cyclic prefix [2] helps in the date rate. The direct consequence is naturally the presence of ISI and ICI components in the received signal which makes the receiver more complicated than that for OFDM. Historically a number of authors proposed and investigated FBMC several decades ago [3]–[5]. The typical modulation used in FBMC is OQAM as opposed to standard QAM. The basic difference in OQAM compared to standard QAM is transmitting symbols as real and imaginary samples and the offset of half of the symbol period between them [6]. The idea is to use two types of orthogonal filter banks, $sine$ and $cosine$ which are generated from a prototype filter investigated in [7]. The complex data symbol is mapped to real symbols, and the orthogonality between carriers and symbols is then required only in the real axis in the case of FBMC.

The pulse shape of the prototype filter for FBMC investigated in [7] is different from the rectangular window used in OFDM and more localized in both frequency and time domain, hence the out of band frequency leakage is minimized. This results in a better modulation technique which provides high spectral efficiency with respect to OFDM. This provides flexibility to use a different pulse shape than the rectangular pulse in OFDM, which is better localized in both frequency and time domains [8]. One such prototype filter known as PHYDYAS filter [9] was presented in [10].

The error floor caused by inter-carrier-interference (ICI) and inter-symbol-interference (ISI) in fading channels is a drawback in FBMC systems, though in AWGN channels these effects are minimal by design. Therefore, receiver processing techniques and precoding techniques to mitigate the effect of ICI and ISI in FBMC systems need to be designed. A two-step algorithm, equalization with interference cancellation (EIC) was proposed in [11], and evaluated for prototype filters derived through the optimization in a single antenna FBMC system. Precoding techniques based on the signal-to-leakage-power-and-noise-ratio (SLNR) for MIMO FBMC systems were presented in [12] and [13]. These, however, have certain limitations in terms of assumptions made and the channels considered. In [14] several linear and non-linear transceiver processing methods were investigated including EIC and Tomlinson Harashima precoding (THP) [15]. In [16] authors propose make-it-real (MIR) precoders with low complexity for OFDM/OQAM.

The existing literature on multiple access schemes includes the following. Authors in [17] considered an uplink scheme based on a multi-mode system with different terminals operating in different modes FBMC, FB-s-FBMC and single carrier (SC) FDMA. In another study [18], a comparison of FBMC and OFDM based uplink schemes was carried out. The work in [19] considers an interference free spatial division multiple

This work has been performed in the framework of the FP7 project ICT-317669 METIS, which is partly funded by the EU.

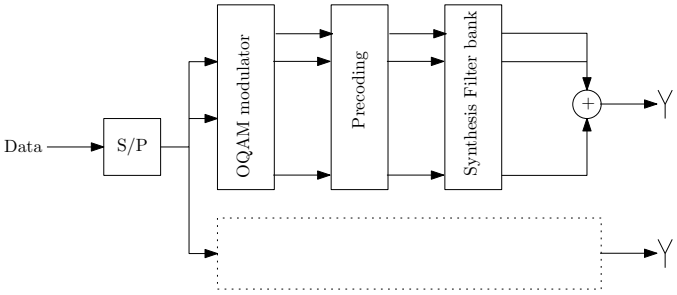

Fig. 1: Transmitter system model

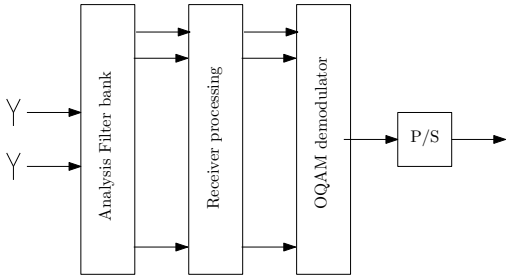

Fig. 2: Receiver system model

access (SDMA) scheme. A modified precoding scheme is investigated for SDMA in [20] whereas a MISO broadcasting scenario is considered by authors in [21].

In this work we evaluate the performance of receiver processing and precoding techniques in MIMO FBMC multiple access systems considering an extended ISI/ICI scenario without simplifications based on a PHYDYAS type filter. The performances of the receiver processing and precoding techniques are examined using the average bit error rate (BER) as the performance metric through simulations.

The rest of this paper is organized as follows. In section II the system model is presented. In section III receiver processing methods and results for the uplink are discussed. Section IV presents precoding techniques and performance for the downlink and Section V concludes the paper.

II. System model

We consider a multicarrier MIMO-FBMC system with $2M$ subcarriers. We consider N_u transmitting users and a single receiver in the uplink, and a single transmitter and N_u receivers in the downlink, each equipped with N_A antennas. Block diagrams of a transmitter and a receiver are given in figures 1 and 2, respectively.

The filter used is $g[k]$ and the filter length is L. We consider a time-invariant Rayleigh fading channel, where the channel delay spread spans Λ sampling intervals. We assume that all antenna paths undergo independent fading. For the receiver processing techniques in the uplink discussed, we assume that the receiver has perfect channel state information (CSI) and the users are synchronized. For the precoding methods in the downlink, we assume that perfect CSI is available at both the transmitter and the receiving users.

A. Uplink

The baseband equivalent transmitted signal from the p-th transmit antenna of the user $u(m)$, who is assigned the m-th band is $s_p^{(m)}[k]$, where the transmitting users employ a real alphabet, and a phase shift equivalent to OQAM modulation [22].

$$\begin{aligned} s_p^{(m)}[k] &= \sum_{n\in\mathbb{Z}} a_{m,n}^{(p)} g[k-nM] e^{j\frac{\pi m}{M}(k-\frac{L-1}{2})} e^{j\phi_{m,n}} \\ &= \sum_{n\in\mathbb{Z}} a_{m,n}^{(p)} g_{m,n}[k] \end{aligned} \tag{1}$$

where $a_{m,n}^{(p)}$ is the real valued transmitted symbol, $g_{m,n}[k] = g[k-nM]e^{j\frac{\pi m}{M}(k-\frac{L-1}{2})}e^{j\phi_{m,n}}$ and $\phi_{m,n} = \frac{\pi}{2}(n+m) - \pi nm$ [22]. The received signal by the q-th receiver antenna from all N_u users, $r_q[k]$,

$$r_q[k] = \sum_{p=1}^{N_A}\sum_{l=0}^{\Lambda-1} h_{p,q}^{(m)}[l] s_p^{(m)}[k-l] + w_q[k] \tag{2}$$

where $h_{p,q}^{(m)}[l]$ is the fading gain of the channel from the $u(m)$-th user in the l-th tap and $w_q[k]$ is the background noise.

$$y_{m',n'}^{(q)} \triangleq \sum_{k\in\mathbb{Z}} r_q[k] g_{m',n'}^*[k] \tag{3}$$

$$\begin{aligned} &= \sum_{p=1}^{N_A}\sum_{m=0}^{2M-1}\sum_{n\in\mathbb{Z}} a_{m,n}^{(p)} e^{j(\phi_{m,n}-\phi_{m',n'}+\pi(m-m')n')} \\ &\times \sum_{l=0}^{\Lambda-1} h_{p,q}^{(m)}[l] e^{-j\frac{\pi ml}{M}} \alpha_g((n'-n)M-l, m-m') \\ &+ \tilde{w}_{m',n'}^{(q)} \end{aligned} \tag{4}$$

where $\alpha_g(x,y) = \sum_{k\in\mathbb{Z}} g[k+x]g[k]e^{j\frac{\pi}{M}(y)(k-\frac{L-1}{2})}$ and $\tilde{w}_{m',n'}^{(q)} = \sum_{k\in\mathbb{Z}} w_q[k] g_{m',n'}^*[k]$.

Using matrix notation to represent the signal from all receiver antenna, we have,

$$\begin{aligned} Y_{m',n'} &= \sum_{m=0}^{2M-1}\sum_{n\in\mathbb{Z}} e^{j(\phi_{m,n}-\phi_{m',n'}+\pi(m-m')n')} \sum_{l=0}^{\Lambda-1} e^{-j\frac{\pi ml}{M}} \\ &\times \alpha_g((n'-n)M-l, m-m') H^{(m)}[l] A_{m,n} + W_{m',n'} \\ &= \sum_{m=0}^{2M-1}\sum_{n\in\mathbb{Z}} e^{j(\frac{\pi}{2}(m-m'+n-n')-\pi(n-n')m)} \sum_{l=0}^{\Lambda-1} e^{-j\frac{\pi ml}{M}} \\ &\times \alpha_g((n'-n)M-l, m-m') H^{(m)}[l] A_{m,n} + W_{m',n'} \end{aligned} \tag{5}$$

where $Y_{m',n'}$ is a length N_A vector, $H^{(m)}[l] = [h_{p,q}^{(m)}[l]]$ is a $N_A \times N_A$ matrix, $A_{m,n} = [a_{m,n}^{(p)}]$ is a length N_A vector and $W_{m',n'} = [\tilde{w}_{m',n'}^{(q)}]$ is a length N_A vector.

We can rewrite $Y_{m',n'}$ as follows,

$$Y_{m',n'} = \sum_{m=0}^{2M-1}\sum_{n\in\mathbb{Z}} H_{m,m-m',n'-n} A_{m,n} + W_{m',n'} \tag{6}$$

where $H_{m,n,m',n'} = e^{j(\frac{\pi}{2}(m-m'+n-n')-\pi(n-n')m)} \sum_{l=0}^{\Lambda-1} H^{(m)}[l] \times \alpha_g((n'-n)M-l, m-m')e^{-j\frac{\pi ml}{M}}$.

B. Downlink

The baseband equivalent transmitted signal from the p-th transmit antenna, $s_p[k]$;

$$\begin{aligned} s_p[k] &= \sum_{m=0}^{2M-1} \sum_{n\in\mathbb{Z}} a_{m,n}^{(p)} g[k-nM] e^{j\frac{\pi m}{M}(k-\frac{L-1}{2})} e^{j\phi_{m,n}} \\ &= \sum_{m=0}^{2M-1} \sum_{n\in\mathbb{Z}} a_{m,n}^{(p)} g_{m,n}[k] \end{aligned} \tag{7}$$

where $a_{m,n}^{(p)}$ is the real valued transmitted symbol, $g_{m,n}[k] = g[k-nM]e^{j\frac{\pi m}{M}(k-\frac{L-1}{2})}e^{j\phi_{m,n}}$ and $\phi_{m,n} = \frac{\pi}{2}(n+m) - \pi nm$. Here, the transmitting user employ a real alphabet, and a phase shift equivalent to OQAM modulation [22]. The received signal by the q-th receiver antenna of the user $u(m')$, who is assigned the m'-th band, $r_q^{(m')}[k]$,

$$r_q^{(m')}[k] = \sum_{p=1}^{N_A} \sum_{l=0}^{\Lambda-1} h_{p,q}^{(m')}[l] s_p[k-l] + w_q^{(m')}[k] \tag{8}$$

where $h_{p,q}^{(m')}[l]$ is the fading gain in the l-th tap of the channel from transmitter to $u(m')$ and $w_q^{(m')}[k]$ is the background noise.

$$\begin{aligned} y_{m',n'}^{(q)} &\triangleq \sum_{k\in\mathbb{Z}} r_q^{(m')}[k] g_{m',n'}^*[k] \\ &= \sum_{p=1}^{N_A} \sum_{m=0}^{2M-1} \sum_{n\in\mathbb{Z}} a_{m,n}^{(p)} e^{j(\phi_{m,n}-\phi_{m',n'}+\pi(m-m')n')} \\ &\times \sum_{l=0}^{\Lambda-1} h_{p,q}^{(m')}[l] e^{-j\frac{\pi ml}{M}} \alpha_g((n'-n)M-l, m-m') \\ &+ \tilde{w}_{m',n'}^{(q)} \end{aligned} \tag{9}$$

where $\alpha_g(x,y) = \sum_{k\in\mathbb{Z}} g[k+x]g[k] e^{j\frac{\pi}{M}(y)(k-\frac{L-1}{2})}$ and $\tilde{w}_{m',n'}^{(q)} = \sum_{k\in\mathbb{Z}} w_q^{(m')}[k] g_{m',n'}^*[k]$.

Using matrix notation to represent the signal from all receiver antenna, we have,

$$\begin{aligned} Y_{m',n'} &= \sum_{m=0}^{2M-1} \sum_{n\in\mathbb{Z}} e^{j(\phi_{m,n}-\phi_{m',n'}+\pi(m-m')n')} \sum_{l=0}^{\Lambda-1} e^{-j\frac{\pi ml}{M}} \\ &\times \alpha_g((n'-n)M-l, m-m') H^{(m')}[l] A_{m,n} + W_{m',n'} \\ &= \sum_{m=0}^{2M-1} \sum_{n\in\mathbb{Z}} e^{j(\frac{\pi}{2}(m-m'+n-n')-\pi(n-n')m)} \sum_{l=0}^{\Lambda-1} e^{-j\frac{\pi ml}{M}} \\ &\times \alpha_g((n'-n)M-l, m-m') H^{(m')}[l] A_{m,n} + W_{m',n'} \end{aligned} \tag{10}$$

where $Y_{m',n'}$ is a length N_A vector, $H^{(m')}[l] = [h_{p,q}^{(m')}[l]]$ is a $N_A \times N_A$ matrix, $A_{m,n} = [a_{m,n}^{(p)}]$ is a length N_A vector and $W_{m',n'} = [\tilde{w}_{m',n'}^{(q)}]$ is a length N_A vector.

We can rewrite $Y_{m',n'}$ as follows,

$$Y_{m',n'} = \sum_{m=0}^{2M-1} \sum_{n\in\mathbb{Z}} \tilde{H}_{m',m,n'-n} A_{m,n} + W_{m',n'} \tag{11}$$

where $\tilde{H}_{m',m,n-n'} = e^{j(\frac{\pi}{2}(m-m'+n-n')-\pi(n-n')m)} \times \sum_{l=0}^{\Lambda-1} H^{(m')}[l] \alpha_g((n'-n)M-l, m-m') e^{-j\frac{\pi ml}{M}}$.

In both the uplink and the downlink, zero forcing (ZF) is used at the receiver, to remove the antenna interference from the output of the synthesis filterbank.

$$\begin{aligned} \tilde{Y}_{m',n'} &= \Re\left\{ \tilde{H}_{m',m',0}^{-1} Y_{m',n'} \right\} \\ &= A_{m',n'} + \Re\Big\{ \sum_{(m,n)\neq(m',n')} \tilde{H}_{m',m',0}^{-1} \tilde{H}_{m',m,n'-n} \\ &\times A_{m,n} \Big\} + \Re\left\{ \tilde{H}_{m',m',0}^{-1} W_{m',n'} \right\} \end{aligned} \tag{12}$$

The interference component $I_{m',n'}$ is given by

$$I_{m',n'} = \Re\left\{ \sum_{(m,n)\in V_{m',n'}} \tilde{H}_{m',m',0}^{-1} \tilde{H}_{m',m,n'-n} A_{m,n} \right\} \tag{13}$$

where the neighborhood of (m',n'), $V_{m',n'} \triangleq \{(m,n) | m,n \in \mathbb{Z}, 0 \le m \le 2M-1, \sum_{l=0}^{\Lambda-1} |\alpha_g((n'-n)M-l, m-m')| > 0, (m,n) \neq (m',n')\}$.

III. Receiver processing in the uplink

A. EIC receiver processing

In this section we look at the performance of equalization with interference cancellation (EIC) method proposed in [11], in a MIMO FBMC system with PHYDYAS filter. Here we first detect the received symbols using zero-forcing. From (6), we have

$$\hat{A}_{m,n}^{(1)} = \mathbb{D}\left[\Re\{H_{m',0,0}^{-1} Y_{m',n'}\}\right] \tag{14}$$

where $\mathbb{D}[\cdot]$ denotes the process of element-wise hard decision demodulation. Then, we use these estimated symbol values ($\hat{A}_{m,n}^{(1)}$) to calculate the ICI and ISI, and remove it from the received signal. Then we again perform zero forcing to obtain a new estimate of the received symbols.

$$\begin{aligned} \hat{A}_{m,n}^{(2)} = \mathbb{D}\Big[\Re\Big\{ H_{m',0,0}^{-1} \big(Y_{m',n'} \\ - \sum_{(m,n)\in V_{m',n'}} H_{m,m-m',n'-n} \hat{A}_{m,n}^{(1)} \big) \Big\} \Big] \end{aligned} \tag{15}$$

We can iterate this process to improve the symbol estimation, at the expense of increased computational complexity and memory. For each additional iteration, we require $N_A^2 |V_{m',n'}|$ additional multiplications to estimate the interference $\sum_{(m,n)\in V_{m',n'}} H_{m,m-m',n'-n} \hat{A}_{m,n}^{(1)}$. Further, if the maximum time index difference of elements in $V_{m',n'}$ is Δn for all (m',n'), the r-th iteration to estimate $\hat{A}_{m',n'}^{(r)}$ requires knowledge of a subset of symbols in the interval $[n' - \frac{\Delta n}{2}, n' + \frac{\Delta n}{2}]$. Hence, the amount of memory required increases linearly with the number of iterations. However, the main performance challenge here is the error propagation. If the initial symbol decision has a lot of errors, the subsequent EIC process is unable to remove the interference.

Simulation results

For the simulations in this section and the subsequent sections, we consider a MIMO system with 2 transmitter and

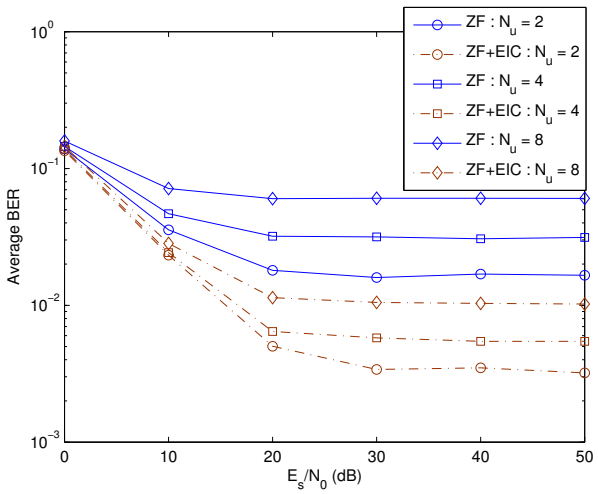

Fig. 3: Average BER with EIC and SEIC ($\Lambda = 2$, $2M = 16$, $L = 63$, $N_A = 2$, $\mathbb{E}\left[h_{p,q}[1]h^*_{p,q}[1]\right] = 0.2$)

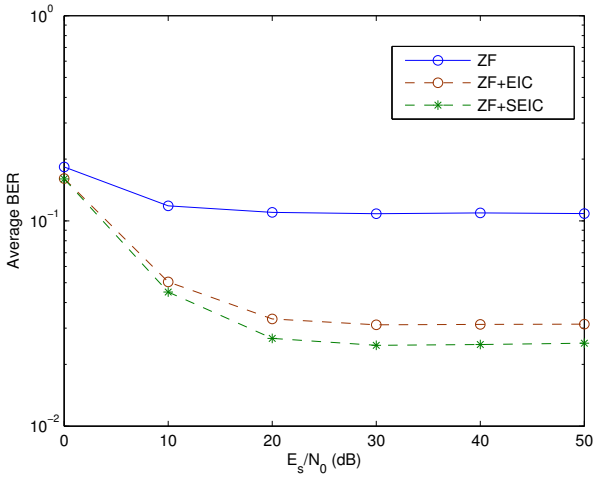

Fig. 4: Average BER with EIC and SEIC ($\Lambda = 2$, $2M = 16$, $L = 63$, $N_A = 2$, $\mathbb{E}\left[h_{p,q}[1]h^*_{p,q}[1]\right] = 0.2$, $N_u = 16$)

receiver antennas ($N_A = 2$) and the number of subcarriers ($2M$) is chosen to be 16. The number of users is N_u. We assign a continuous block of $\frac{2M}{N_u}$ subcarriers to each user. We assume that the channel between p-th transmitter antenna and the q-th receiver antenna is a two-path time-invariant Rayleigh channel. The average gain of the first path is assumed to be unity; i.e. $\mathbb{E}\left[h_{p,q}[0]h^*_{p,q}[0]\right] = 1$.

Fig. 3 shows the average bit error rate (BER) of the uplink with EIC processing at the receiver, parameterized by the number of users N_u. We have plotted the average BER with only the removal of antenna interference by ZF as shown in Eq. (12) for comparison. The number of channel taps $\Lambda = 2$, $\mathbb{E}\left[h_{p,q}[1]h^*_{p,q}[1]\right] = 0.2$ and the number of iterations of EIC processes is 2.

We note that larger the number of users, the higher the performance error floor in the system. As can be seen from the analysis in section II-A, if the phase of the channel fading in all subcarriers was equal, we can remove all the interference from adjacent subcarriers. Similarly, if the phase of the channel fade is significantly different between adjacent subcarriers, the more significant the inter carrier interference is. Hence, when we have more users sharing the subcarriers, and since the channel from each user to the uplink is mutually independent, the interference between subcarriers is going to be larger. Therefore, the error floor increases with N_u.

B. Successive EIC

In order to improve the initial detection, we can start from the user with the least amount of interference and proceed to users with higher levels of interference, when performing the EIC. We call this ordered processing successive EIC (SEIC). The metric we use to select the order of users (m') for processing is $\left\| \Re\left\{ H^{-1}_{m',0,0} \sum_{(m,n)\in V_{m',n'}} H_{m,m-m',n'-n} \right\} \right\|_1$, which relate to the worst case interference from adjacent symbols to the symbols in the user m'.

Simulation results

Fig. 4 shows the average bit error rate (BER) of the uplink with EIC and SEIC processing at the receiver. We have plotted the average BER with only the removal of antenna interference by ZF as shown in Eq. (12) for comparison. The number of channel taps $\Lambda = 2$, $\mathbb{E}\left[h_{p,q}[1]h^*_{p,q}[1]\right] = 0.2$ and the number of iterations of EIC and SEIC processes is 2. We note that the system has an error floor larger than 10^{-1} with ZF, which is due to the increased ICI caused by different channel fading phases undergone by the users in adjacent subcarriers. The EIC receiver processing has lowered the error floor close to 2×10^{-2}. We note that SEIC can further lower the error floor.

C. Error correction coding

Forward error correction (FEC) can be used in attempt to remove the error floor by improving the accuracy of the initial symbol estimation $\hat{A}^{(1)}_{m,n}$. Here we make use of convolutional codes. Fig. 5 shows the basic receiver model.

Simulation results

Fig. 6 shows the average BER when convolution code based FEC is used in conjunction with EIC and SEIC. We have evaluated performance with a rate $\frac{1}{2}$ convolutional code with memory 6. For comparison, average BER without EIC is also presented. When compared with the results in Fig. 3, we note that the error floor can be significantly lowered with the use of the rate $\frac{1}{2}$ convolutional code.

D. Channel allocation

In the uplink, the level of ICI is significant because the signals from different users in adjacent subcarriers has different channel fading phases. We assume the channel allocation is done by the receiver, who has CSI of all the links. The interference from the user in subcarrier m to user in m' is given by $\Re\left\{ H^{-1}_{m',0,0} H_{m,m-m',n'-n} \right\} A_{m,n}$. Hence, we know that $\left\| \Re\left\{ H^{-1}_{m',0,0} H_{m,m-m',n'-n} \right\} \right\|_1$ is an upper bound to the sum of the interference from m to m', on all antennas.

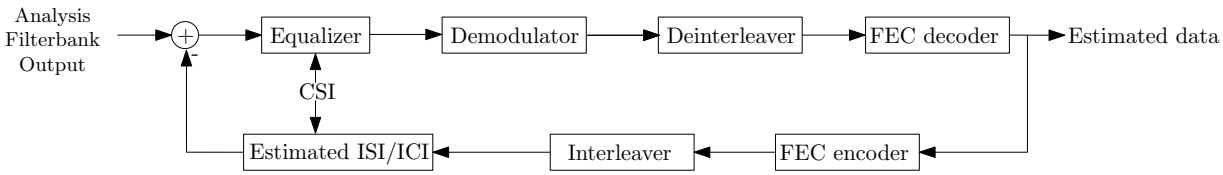

Fig. 5: Receiver system model incorporating FEC with EIC

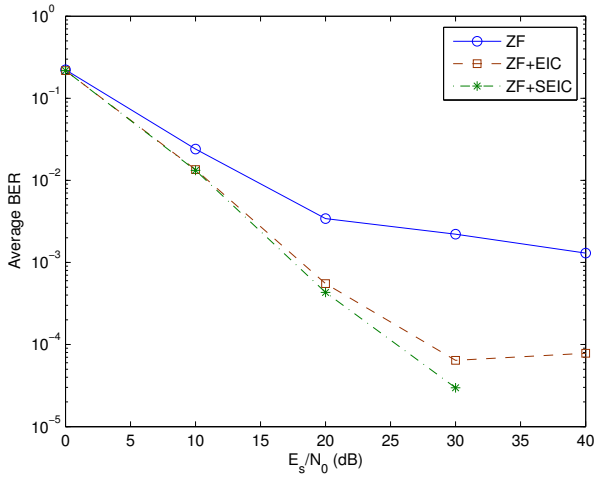

Fig. 6: Average BER of EIC and SEIC with FEC ($\Lambda = 2$, $2M = 16$, $L = 63$, $N_A = 2$, $\mathbb{E}\left[|h_{p,q}[1]|^2\right] = 0.2$, $N_u = 2$)

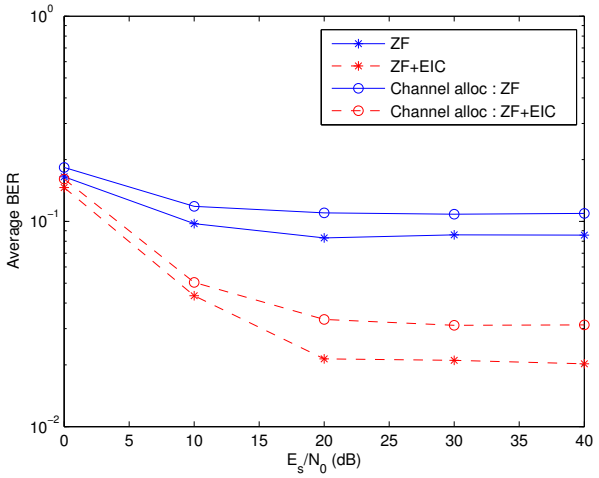

Fig. 7: Average BER with EIC with channel allocation ($\Lambda = 2$, $2M = 16$, $L = 63$, $N_A = 2$, $\mathbb{E}\left[|h_{p,q}[1]|^2\right] = 0.2$, $N_u = 16$)

In allocating channels among users, we allocate the first subcarrier to a user arbitrary. Then each subsequent subcarrier is assigned to one of the remaining users who has the minimum interference upper bound to the previous subcarrier.

Simulation results

Fig. 7 shows the average BER with and without EIC processing, when using the channel allocation in conjunction. For comparison, average BER without channel allocation is also presented. We note that in Fig. 7, the channel allocation algorithm lowers the error floor slightly.

IV. Precoding at the Transmitter for the Downlink

A. THP precoding

At the transmitter, the expected interference due to ICI and ISI is calculated using (13). And we update the transmitted symbols to cancel the possible expected interference. Hence, the transmitted symbols can be written as

$$\overline{A}^{(1)}_{m',n'} = A_{m',n'} - \Re\Big\{ \sum_{(m,n)\in V_{m',n'}} \tilde{H}^{-1}_{m',m',0} \tilde{H}_{m',m,n'-n} A_{m,n} \Big\}. \tag{16}$$

However, since the interference occur from symbols transmitted both prior to and after from each symbol, the updating of the symbol in position (m', n') affects its interference to symbols transmitted prior to it. Hence, the technique in (16) cannot completely remove the interference. We can further iterate this process to improve the interference cancellation, incurring higher computational complexity and memory requirements, similar to EIC in section III-A.

$$\overline{A}^{(r+1)}_{m',n'} = \overline{A}^{(r)}_{m',n'} - \sum_{(m,n)\in V_{m',n'}} \Re\Big\{ \tilde{H}^{-1}_{m',m',0} \tilde{H}_{m',m,n'-n} \Big\} \times \left(\overline{A}^{(r)}_{m,n} - \overline{A}^{(r-1)}_{m,n} \right) \tag{17}$$

Simulation results

The average BER of the MIMO FBMC system with THP precoding to cancel the interference is presented in Fig. 8. The performance without precoding is plotted for comparison.

We note that the precoding technique in (16) has reduced the error floor in the MIMO FBMC system. However, this does not offer significant performance improvement over ZF. This is because the precoding technique in (16) cannot completely remove the interference, as discussed earlier. Further, we can see that the increase in the number of users had not affected the performance significantly, which was the case for the uplink in Fig. 3. This is because in the downlink, at the receiver, the time domain fading of the channel is the same in all subcarriers, irrespective of the number of users sharing the subcarriers. Hence, the level of inter carrier interference is unaffected by N_u, unlike in the uplink.

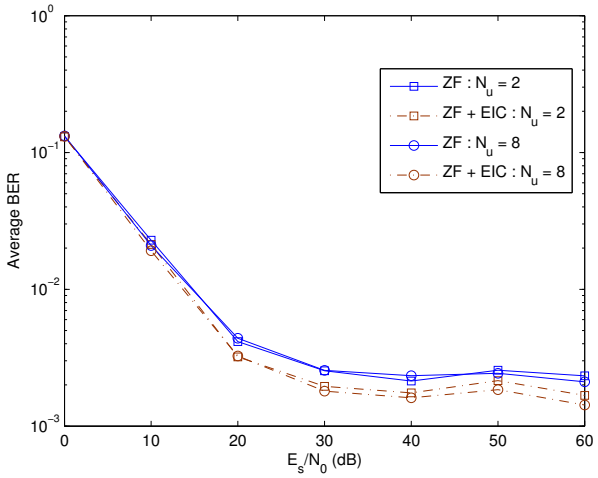

Fig. 8: Average BER with THP ($\Lambda = 2$, $2M = 16$, $L = 63$, $N_A = 2$, $\mathbb{E}\left[|h_{p,q}[1]|^2\right] = 0.2$)

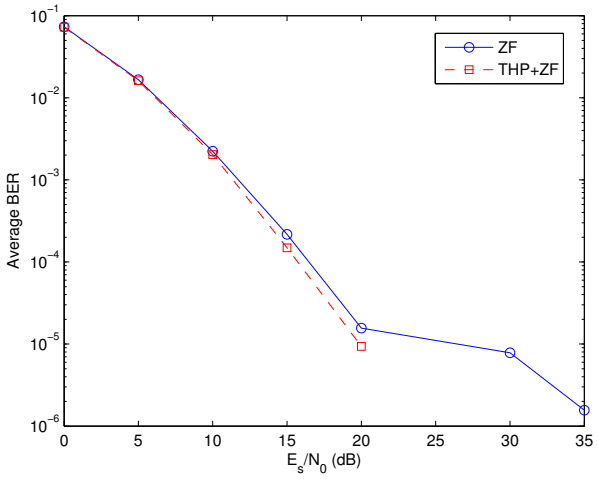

Fig. 9: Average BER with THP precoding and channel allocation ($\Lambda = 2$, $2M = 16$, $L = 63$, $N_A = 2$, $\mathbb{E}\left[|h_{p,q}[1]|^2\right] = 0.2$, $N_u = 16$)

B. THP with channel allocation

The interference to the (m', n') symbols from $A_{m,n}$ is given by $\Re\left\{H^{-1}_{m',m',0} H_{m',m,n'-n} A_{m,n}\right\}$ as shown in (13). Define $\hat{H}_{m',m,n'-n} \triangleq \text{abs}\left[\Re\left\{H^{-1}_{m',0,0} H_{m,m-m',n'-n}\right\}\right]$, where abs$[\cdot]$ is the elementwise absolute value.

We have the following elementwise inequality,

$$\tilde{H}_{m',m,n'-n} \mathbf{1}_{N_A \times 1} \geq \Re\left\{H^{-1}_{m',m',0} H_{m',m,n'-n}\right\} A_{m,n} \quad (18)$$

where we assume transmitted symbols have unit energy and $\mathbf{1}_{N_A \times 1}$ is a length N_A column vector with unit valued elements. This implies $\hat{H}_{m',m,n'-n}\mathbf{1}_{N_A \times 1}$ gives an upper bound to the interference from $A_{m,n}$. This upper bound is dependent only on the channel of the m'-th user. Therefore, we can calculate upper bounds for the interference for all users independently of the channel allocation of the rest of users. We can use these upper bounds to allocate channels across users.

We minimize the objective parameter $\sum_{(m,n)\in V_{m',0}} \|\hat{H}_{m',m,-n}\|_1$, $\forall m' \in \{0, 1, \ldots, 2M-1\}$, to find the optimal channel allocation.

Simulation results

The average BER with the channel allocation with and without THP precoding is given in Fig. 9. Comparing the results without the use of channel allocation algorithm in Fig. 8, we note that the channel allocation algorithm lowers the error floor below 10^{-5} without the use of any precoding. The precoding appears to help even further lower the error rate.

V. Conclusion

In this paper we evaluated the performance of transceiver processing techniques to improve the average BER of multiuser MIMO FBMC systems. For the uplink several schemes were considered based on zero forcing and equalization with interference cancellation. The performance results show that there is an error floor due to interference components present, which can be significantly lowered or removed by forward error correction methods. For the downlink, the results are much better and precoding improves performance further.

References

[1] B. Le Floch, M. Alard, and C. Berrou, "Coded orthogonal frequency division multiplex [tv broadcasting]," *Proceedings of the IEEE*, vol. 83, no. 6, pp. 982 – 996, 1995.

[2] N. Zorba, S. Pfletschinger, and F. Bader, "Increasing the performance of ofdm-oqam communication systems through smart antennas processing," in *First International ICST Conference, MOBILIGHT 2009, Athens, Greece*, May 2009.

[3] B. Hirosaki, "An orthogonally multiplexed qam system using the discrete fourier transform," *IEEE Trans. Commun.*, vol. 29, pp. 982–989, 1981.

[4] R. W. Chang, "Synthesis of band-limited orthogonal signals for multichannel data transmission," *Bell Syst. Tech. J.*, vol. 45, pp. 1775–1796, 1966.

[5] B. R. Saltzberg, "Performance of an efficient parallel data transmission system," *IEEE Trans. Commun. Technol.*, vol. 15, pp. 805–811, 1967.

[6] H. Bölcskei, "Orthogonal frequency division multiplexing based on offset qam,chapter in advances in gabor analysis."

[7] M. Bellanger, "Physical layer for future broadband radio systems," in *IEEE Radio and Wireless Symposium (RWS)*, 2010, pp. 436–439.

[8] B. Farhang-Boroujeny, "Ofdm versus filter bank multicarrier," *IEEE Signal Processing Magazine*, vol. 28, no. 3, pp. 92–112, 2011.

[9] "Physical layer for dynamic spectrum access and cognitive radio (phydyas)," *7th Framework Programme project http://www.ict-phydyas.org/*, 2010.

[10] M. Bellanger, "Specification and design of a prototype filter for filter bank based multicarrier transmission," in *IEEE International Conference on Acoustics, Speech, and Signal Processing, 2001. Proceedings. (ICASSP '01). 2001*, vol. 4, 2001, pp. 2417–2420 vol.4.

[11] H. Lin, C. Lele, and P. Siohan, "Equalization with interference cancellation for hermitian symmetric ofdm/oqam systems," in *IEEE International Symposium on Power Line Communications and Its Applications, 2008. ISPLC 2008.*, 2008, pp. 363–368.

[12] U. Jayasinghe, N. Rajatheva, and M. Latva-aho, "Application of a leakage based precoding scheme to mitigate intrinsic interference in fbmc," in *IEEE International Conference on Communication*, June 2013.

[13] ——, "Leakage based multi user beamforming scheme to mitigate interference in mimo-fbmc," in *WSA 2013 - 17th International ITG Workshop on Smart Antennas*, March 2013.

[14] M. Soysa, N. Rajatheva, and M. Latva-aho, "Linear and non-linear transceiver processing for mimo-fbmc systems," in *IEEE International Conference on Communication*, June 2014.

[15] C. Windpassinger, R. F. H. Fischer, T. Vencel, and J. Huber, "Precoding in multiantenna and multiuser communications," *IEEE Transactions on Wireless Communications*, vol. 3, no. 4, pp. 1305–1316, 2004.

[16] D.-T. Phan-Huy, Baltar, P. Siohan, and M. Hlard, "Make-it-real precoders for mimo ofdm/oqam without inter carrier interference," in *IEEE Globecom 2013*, 2013.

[17] T. Ihalainen, A. Viholainan, T. H. Stitz, M. Renfors, and M. Bellanger, "Filter bank based multi-mode multiple access scheme for wireless uplink," pp. 1354–1358, 2009.

[18] H. Saeedi-Sourck, Y. Wu, M.-B. Jan, W., S. Sadri, and B. Farhang-Boroujeny, "Complexity and performance comparison of filter bank multicarrier and ofdm in uplink of multicarrier multiple access networks," *IEEE Transactions on Signal Processing*, vol. 59, no. 4, pp. 1907–1912, 2011.

[19] F. Horlin, J. Fickers, T. Deleu, and J. Louveaux, "Interference-free sdma for fbmc-oqam," *EURASIP Journal on Advances in Signal Processing*, vol. 2013, 2013.

[20] M. Caus and A. Perez-Neira, "Sdma for filterbank with tomlinson harashima precoding," in *Communications (ICC), 2013 IEEE International Conference on*, 2013, pp. 4571 – 4575.

[21] M. Newinger, L. G. Baltar, A. L. Swindlehurst, and J. A. Nossek, "Miso broadcasting fbmc system for highly frequency selective channels," in *Smart Antennas (WSA), 2014 18th International ITG Workshop on*, 2014, pp. 1–7.

[22] P. Siohan, C. Siclet, and N. Lacaille, "Analysis and design of ofdm/oqam systems based on filterbank theory," *IEEE Transactions on Signal Processing*, vol. 50, no. 5, pp. 1170–1183, 2002.